

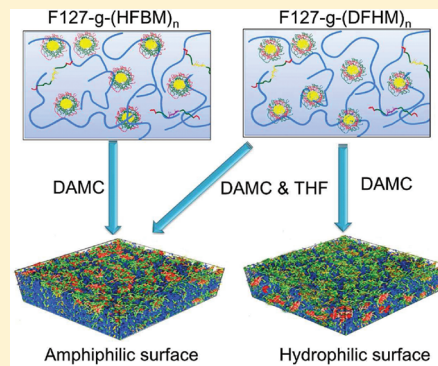
Efficient Wastewater Treatment by Membranes through Constructing Tunable Antifouling Membrane Surfaces

Wenjuan Chen,[†] Yanlei Su,[†] Jinming Peng,[†] Xuetong Zhao,[†] Zhongyi Jiang,^{*,†} Yanan Dong, Yan Zhang,[†] Yangui Liang,[†] and Jiazen Liu[†]

[†]Key Laboratory for Green Chemical Technology of Ministry of Education, School of Chemical Engineering and Technology, Tianjin University, Tianjin 300072, P. R. China

 Supporting Information

ABSTRACT: In the present study, a facile *in situ* approach for constructing tunable amphiphilic or hydrophilic antifouling membrane surfaces was demonstrated by exquisitely manipulating the microphase separation and surface segregation behavior of the tailor-made ternary amphiphilic block copolymers during the commonly utilized wet phase inversion membrane-formation process. Under dead-end filtration for oily wastewater treatment, the membrane with amphiphilic surface exhibited over 99.5% retention ratio of chemical oxygen demand (COD) without appreciable membrane fouling; the water permeation flux was slightly decreased during operation (total flux decline was 6.8%) and almost completely recovered to the initial value (flux recovery ratio was more than 99.0%) after simple hydraulic washing. While for the proteins-containing wastewater treatment, the membrane with hydrophilic surface exhibited about 52.6% COD retention ratio and superior antifouling performance: only 17.0% total flux decline and also more than 99.0% flux recovery ratio. Hopefully, the present approach can be developed as a competitive platform technology for the preparation of robust and versatile antifouling membrane, leading to the high process efficiency of wastewater treatments.



1. INTRODUCTION

Large amounts of wastewater are generated each day by hydrocarbon processing, metallurgical, pharmaceutical, and food industries, etc., rendering a promising source of water for beneficial use.^{1–4} Owing to the inherent advantages, membrane technology emerges as a highly competitive candidate for reclamation and reuse of water, capturing water directly from such nontraditional sources and restoring it to potable or irrigation quality water.^{1,3–6} However, when incorporated in wastewater treatment processes, the semipermeable membrane systems offer high surface areas for attachment of numerous foulants. Besides, unlike the nonporous coatings, the foulants may block inside the membrane pores. Severe membrane fouling inevitably occurs, and the consequences are detrimental: significantly reduced flux, poor separation efficiency, product contamination, frequent cleaning, accelerated aging due to aggressive cleaning regimes, and membrane damage.^{1,8–9}

Increasingly, extensive environmental concerns trigger a number of antifouling chemistries. In view of the construction for antifouling porous membrane surfaces, surface segregation coupled with the commercially utilized wet phase inversion membrane-formation process has been developed as an *in situ* and three-dimensional alternative for generating more efficacious antifouling brush layers, without the drawbacks of traditional surface coating and surface grafting methods, such as reducing intrinsic permeability owing to partial pore blockage, unable to modify the internal

pores, needing an extra manufacturing step.^{1,9–11} So far, a majority of the research focuses on constructing hydrophilic antifouling membrane surfaces, which possess single chemical architecture of hydrophilic characteristics. Specific copolymers, comprising hydrophilic and hydrophobic segments, are incorporated into the casting solution as versatile additives. The hydrophobic segments in such amphiphilic copolymers ensure a strong “anchoring” within the polymer bulk matrix, while the hydrophilic segments segregate freely onto polymer/water interface.^{1,10,11} The resultant hydrophilic microdomains could generate a compact hydration layer on the surface through hydrogen or ionic bonding, exhibiting superior “fouling resistant” property and effectively preventing the nonspecific adsorption of biofoulants.^{12–18} In our recent study, amphiphilic antifouling membrane surfaces, which possess mixed architecture of mosaic hydrophilic and low surface energy characteristics, were constructed with fluorine-containing copolymers by a “forced surface segregation” method.⁹ However, in the membrane water treatment industries, the surface foulants mainly included four classes: proteins, natural organic matter, extracellular polymeric substances, and oil (hydrocarbons). Different kinds of foulants require different surface antifouling architecture.^{9,15,18}

Received: March 27, 2011

Accepted: June 28, 2011

Revised: June 23, 2011

Published: June 28, 2011

A facile and generic approach for constructing tunable antifouling surfaces to deter different foulants is an imperative and pervasive demand, doubtlessly. Besides, universally applicable additives for the modification of wide-spectrum membrane matrix materials will provide a competitive platform technology for generating variable and multifunctional antifouling surfaces.

In general, the whole wet phase inversion membrane-formation process involves two crucial steps: preparation of polymer casting solution and subsequent phase inversion of the solution-cast polymer film.^{19,20} Spontaneous microphase separation of the amphiphilic copolymers takes place in the first step, whereas surface segregation occurs in the second step. When dissolved into a specific solvent, the amphiphilic copolymers form structures with certain exterior boundaries response or adapt to the solvent for achieving thermodynamic equilibrium state.^{21–23} Theoretically, both microphase separation and surface segregation behaviors of the amphiphilic copolymers can be tuned by the copolymer conformation type and structure, solvent nature, and composition, etc. Intensive insight into the relevant mechanism behind the two behaviors will be profitable to explore the full potential of the whole wet phase inversion membrane-formation process for *in situ* control over the surface architecture.

Here, a facile strategy for constructing tunable amphiphilic or hydrophilic antifouling membrane surfaces was demonstrated for effectively combating different surface foulants. A standard engineering polymer, polyvinylidene fluoride (PVDF), was utilized as membrane bulk material, novel ternary amphiphilic block copolymers composed of hydrophobic “anchoring” block, hydrophilic “fouling resistant” block, and nonpolar hydrophobic (low surface energy) “fouling release” block tethered at both ends were utilized as additives. By varying the copolymers conformation and the solvent volatility in the casting solution, we can flexibly manipulate the microphase separation and surface segregation of the ternary amphiphilic copolymers during membrane-formation process, in pursuit of tunable antifouling surfaces. The surface construction was affirmed by the X-ray photoelectron spectroscopy (XPS) and atomic force microscopy (AFM). Using the oil/water emulsion, protein aqueous solution as model foulants, the separation properties of the membranes were extensively investigated, and the antifouling properties, fouling resistant and fouling release properties were tentatively correlated with several surface attributes.

2. METHODS

2.1. Ternary Amphiphilic Copolymers Synthesis. The ternary amphiphilic copolymers were prepared via cerium ion redox system initiated soap-free emulsion polymerization based on the commercial PEO-PPO-PEO (Pluronic F127) triblock copolymer and side-chain fluorinated methacrylate monomer (hexafluorobutyl methacrylate (HFBM) or dodecafluoroheptyl methacrylate (DFHM)). The as-synthesized copolymers were designated as F127-g-(HFBM)_n or F127-g-(DFHM)_n, where “n” represented the unit number of HFBM or DFHM calculated based on the actual synthesis formulation. The structure and chemical compositions of the copolymers were confirmed by Fourier transform infrared (FTIR) (Nicolet S60) and ¹H NMR (INVOA-500) characterization.

2.2. Membrane Preparation. All the membranes were prepared through the wet phase inversion process with PVDF as bulk material, single *N,N*-dimethylacetamide (DAMC) or a mixture of tetrahydrofuran (THF) and DMAC as solvent (weight ratio of

THF and DMAC was 1:4), the ternary amphiphilic copolymers as additive, and water as the nonsolvent coagulation bath. The weight percentages of PVDF and amphiphilic copolymers in solvent were 16 wt % and 8 wt %, respectively. The casting solutions were stirred for 4 h at 60 °C and then left for 6 h to allow complete release of bubbles. Then, the casting solutions were spread with a casting knife and immersed in a water coagulation bath. The resultant membranes were designated as PVDF/X~Y membranes, where X and Y indicated the selected additive and solvent during the membrane preparation process, respectively. The PVDF/PEG2000~DMAC membrane was prepared as control membrane following the similar procedure.

The cross-section and surface morphologies of the membranes were observed by scanning electron microscopy (SEM) (Philips XL30E scanning microscope) and AFM characterization (Agilent Technologies 5500). The membrane surface compositions were analyzed by XPS (PHI-1600). Contact angle analysis upon membrane surfaces was conducted by a contact angle goniometer (JC2000C Contact Angle Meter). The surface free energy, γ , was calculated using the three-liquid Lifshitz-van der Waals acid–base model, with two polar liquids (water and glycerol) and one apolar liquid (diiodomethane) as test liquids.

2.3. Separation Properties Evaluation. A dead-end stirred cell (model 8200, Millipore Co.) filtration system connected with a nitrogen gas cylinder and solution reservoir was adopted to characterize the permeation, retention, and antifouling properties of the membranes. The filtration were carried out at room temperature of 25 ± 1 °C with a near-surface stirring speed of 200 rpm. The model feed solutions included oil/water emulsion (GS-1 high-speed vacuum pump oil, 1000 ppm; SDS as emulsifier, 100 ppm. The emulsions were used within 24 h.) and BSA aqueous solution (1000 ppm; pH value was 7 adjusted by phosphate buffer solution).

Each membrane was initially pressurized at 0.1 MPa for 1 h, and then the operation pressure was set at 0.05 MPa. The definition of water flux J_{w1} (L/(m²h)) was the same as previously reported.⁹ Then, stirred cell and solution reservoir were emptied and refilled with model feed solution. The flux for feed solutions J_p (L/(m²h)) was measured based on the water quantity permeating the membranes. The retention ratios of oil and BSA were calculated by determining the corresponding concentration in the feed and permeate solutions by UV-spectrophotometer (UV-9200) at wavelengths of 531 and 278 nm, respectively. The chemical oxygen demand (COD) and turbidity were measured using Lovibond ET 99722 Fast COD Detection Instrument and Shangke WGZ-100 Digital Photoelectrical Turbidimeter, respectively. After filtration of feed solution, the membranes were washed with deionized water for about 20 min, and then water flux of cleaned membranes J_{w2} (L/(m²h)) was remeasured.

3. RESULTS AND DISCUSSION

3.1. Controllable Ternary Amphiphilic Copolymer Synthesis. The ternary amphiphilic copolymers were specifically designed which consisted of hydrophobic PPO, hydrophilic PEO, and nonpolar hydrophobic (low surface energy) fluorine-containing (PHFBM or PDFHM) blocks. The synthesis was conducted via nonsoap free radical copolymerization using a cerium ion redox system as initiator in aqueous solution. Each Pluronic F127 molecule bore two carbon atoms linked with hydroxyl groups at each chain end, which could be activated by the redox reaction between cerium ions (IV) and CH–OH groups.

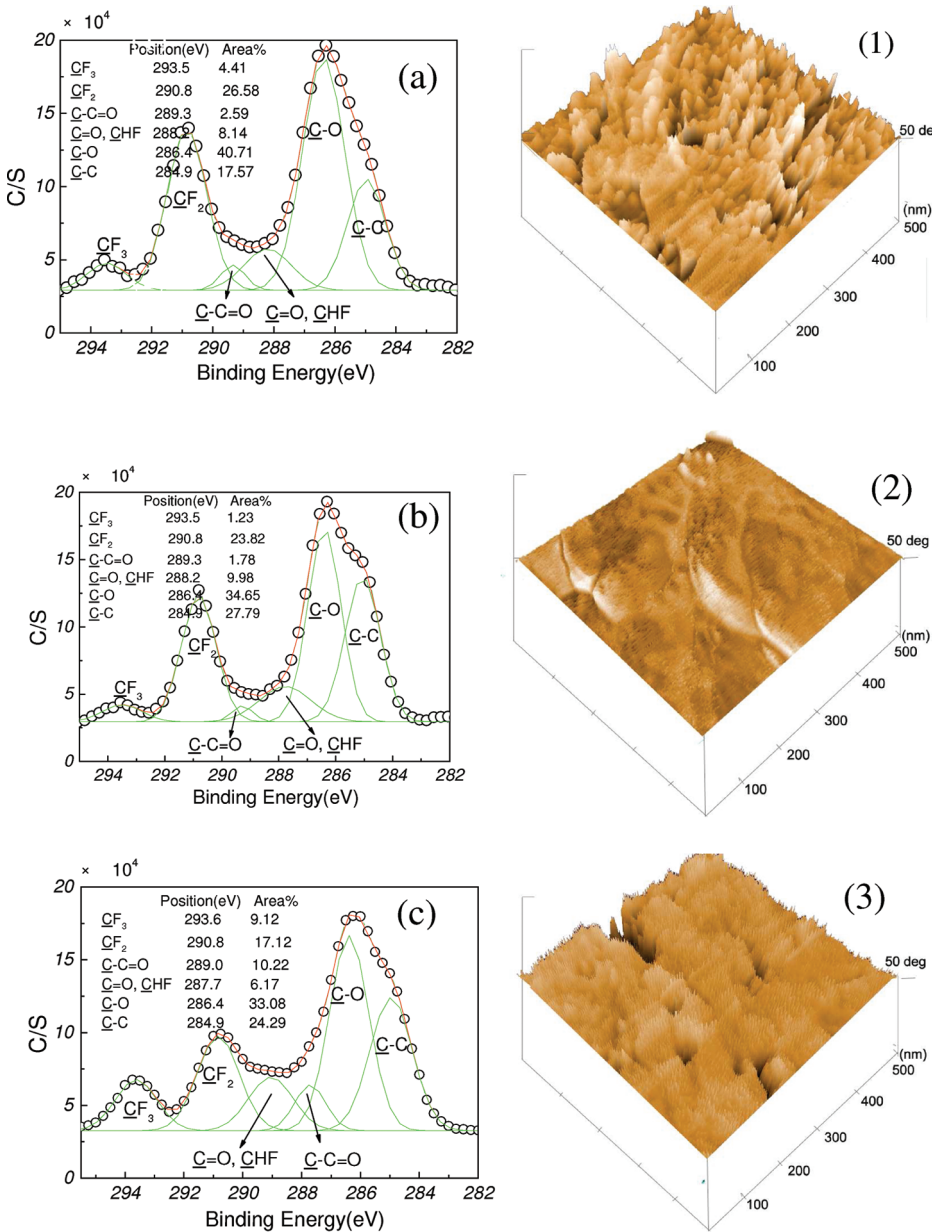


Figure 1. XPS C1s core level spectra resolving results of (a) PVDF/F127-g-(HFBM)₈~DMAC, (b) PVDF/F127-g-(DFHM)₈~DMAC, and (c) PVDF/F127-g-(DFHM)₈~DMAC and THF membranes. The surface AFM phase images (500×500 nm) for (1) PVDF/F127-g-(HFBM)₈~DMAC, (2) PVDF/F127-g-(DFHM)₈~DMAC, and (3) PVDF/F127-g-(DFHM)₈~DMAC and THF membranes. The vertical scale was 50 degrees.

The resultant radicals on those carbon atoms favored the grafting copolymerization of fluorine-containing acrylate monomers, that is, HFBM or DFHM monomers. Finally, ternary pentablock copolymers, PHFBM-PEO-PPO-PEO-PHFBM or PDFHM-PEO-PPO-PEO-PDFHM, were obtained, which were simplified as F127-g-(HFBM)_n or F127-g-(DFHM)_n, n = 2, 4, 8, 20, representing the theoretical unit number of HFBM or DFHM calculated from the synthesis formulation assuming a 100% grafting efficiency. The successful copolymerization was verified by FTIR and ¹H NMR characterization (see Figure S1 and Table S1, Supporting Information).

3.2. Tunable Antifouling Surfaces Construction. Typically, the wet phase inversion process generated asymmetric membranes. In this study, compared with control PVDF membrane, all the membranes exhibited the similar cross-sectional morphologies with

amounts of fully developed macropores beneath the top layer (see Figure S2, Supporting Information), indicating that the incorporation of ternary amphiphilic copolymers exerted little influence on the membrane-forming property of PVDF material. The modified membranes possessed much more narrow pore size distribution compared with the control PVDF membranes (ranging from 20 to 100 nm), positioning the membranes in the range of ultra- to microfiltration.

Synchronizing with the membrane formation process, tunable antifouling surface constructions were accomplished. Copolymer conformation and solvent volatility were chosen as principal regulation variables for the microphase separation and surface segregation.

Regulation via Ternary Amphiphilic Copolymer Conformation. When amphiphilic copolymers, which were composed of

Table 1. Surface Coverage Ratio of Each Block from the Ternary Amphiphilic Copolymers on Membrane Surfaces

entry	membranes	surface coverage of each block [%]			
		Φ_{HFBM}/Φ_{DFHM}	Φ_{PEO}	Φ_{PPO}	Φ_{matrix}
1	PVDF/PEG2000~DMAC	---	13.8	4.6	81.5
2	PVDF/F127-g-(HFBM) ₂ ~DMAC	18.3	20.0	6.6	55.1
3	PVDF/F127-g-(HFBM) ₄ ~DMAC	39.4	30.6	10.2	19.8
4	PVDF/F127-g-(HFBM) ₈ ~DMAC	35.2	36.5	12.1	16.2
5	PVDF/F127-g-(HFBM) ₂₀ ~DMAC	30.2	29.7	9.9	30.2
6	PVDF/F127-g-(DFHM) ₂ ~DMAC	8.6	15.2	5.1	71.1
7	PVDF/F127-g-(DFHM) ₄ ~DMAC	7.4	26.7	8.9	57.0
8	PVDF/F127-g-(DFHM) ₈ ~DMAC	3.0	35.3	11.7	50.0
9	PVDF/F127-g-(DFHM) ₂₀ ~DMAC	2.9	32.9	11.0	43.0
10	PVDF/F127-g-(DFHM) ₂ ~DMAC and THF	23.1	14.0	4.6	58.3
11	PVDF/F127-g-(DFHM) ₄ ~DMAC and THF	28.4	22.1	7.4	42.1
12	PVDF/F127-g-(DFHM) ₈ ~DMAC and THF	33.5	30.2	10.0	26.3
13	PVDF/F127-g-(DFHM) ₂₀ ~DMAC and THF	18.2	17.8	5.9	58.1

covalently bonded but mutually incompatible constituent blocks, dissolved into certain solvent, the microphase separation occurs: forming certain structures with strong solvophilic blocks exposed to polymer/solvent interfaces for achieving minimal interface energy.^{21–23}

DMAC was first utilized as the membrane casting solvent due to its good dissolving ability for the membrane bulk material PVDF. A distinct microphase separation of the ternary amphiphilic copolymers ($F127-g-(HFBM)_n$ or $F127-g-(DFHM)_n$) in DMAC were anticipated due to the diverse affinities toward the solvent of their constituent blocks. Accordingly, the microphase separation of the ternary amphiphilic copolymers mainly fell into two catalogues:²² (i) microphase separation of ternary amphiphilic copolymers as a whole from the membrane bulk material, i.e. PVDF, and (ii) microphase separation of the blocks with each other inside the ternary amphiphilic copolymers (see Figure S3, Supporting Information). The solubility parameters (δ) of PPO, PEO, PHFBM, and PDFHM blocks were about 8.6, 9.4, 11.9, and 13.3 (cal/cm²)⁻³, respectively, whereas 11.1 (cal/cm²)⁻³ for DMAC. Based on the solubility parameter theory, the PHFBM blocks may reside at the exterior boundaries of the $F127-g-(HFBM)_n$ clusters and expose to the solvent, while PDFHM blocks may be hidden inside the $F127-g-(DFHM)_n$ clusters (see Figure S3, Supporting Information). Hence, it could be envisioned that during the subsequent phase inversion process, PHFBM blocks were more easily segregated onto the polymer–water interface compared with the PDFHM blocks, resulting in versatile antifouling membrane surfaces.

XPS and AFM were employed to probe the chemical feature of the membrane surfaces. Three characteristic signals for carbon, oxygen, and fluorine in the XPS spectra were clearly observed on all the membrane surfaces. To provide more detailed surface composition, XPS C1s core level spectra were resolved into six peaks representing different chemical environments using a sum of Lorentzian–Gaussian functions. Exemplarily, the resolving results for PVDF/F127-g-(HFBM)₈~DMAC and PVDF/F127-g-(DFHM)₈~DMAC membranes were presented in Figure 1 (a) and (b). As PHFBM/PDFHM blocks were the only source of CF_3 , the surface coverage ratios of PHFBM/PDFHM blocks (Φ_{HFBM}/Φ_{DFHM}) were calculated directly from the CF_3 area percentages according to the above data, and the corresponding

information was listed in Table 1, entries 2–9. Accordingly, the surface coverage of PEO blocks (Φ_{PEO}) was calculated.

With the increase of grafting degree of HFBM or DFHM in the ternary amphiphilic copolymer, both Φ_{HFBM} and Φ_{PEO} values for all the membranes showed a similar changing trend: increase initially but then decrease, which could be explained by the contribution of entropic factor for the ternary amphiphilic copolymers surface segregation behavior: short length moieties tend to segregate to the interface for losing the least entropy. With $F127-g-(HFBM)_n$ as additives, the Φ_{PEO} and Φ_{HFBM} values reached the maximum values of 36.5% and 35.2%, which were dramatically enhanced compared with the theoretical values calculated from the actual copolymers composition and membrane formation recipe (data were not shown here). Therefore, the anticipated amphiphilic membrane surfaces were acquired. Meanwhile, with $F127-g-(DFHM)_n$ as additives, the values of Φ_{PEO} were enhanced remarkably compared with the theoretical values with a maximum value of 35.3% (Table 1, entries 6–9), whereas the Φ_{DFHM} values were changed only slightly and retained at a relative low level, leading to the formation of hydrophilic membrane surfaces.

AFM phase images provided height resolutions at the surfaces, as morphological indication for surface chemical composition changes. The observations were performed in a scan size of 500 × 500 nm from the nonporous part of the membrane surface. Compared with hydrophilic PVDF/F127-g-(DFHM)₈~DMAC membrane surface (Figure 1 (2)), the surface corrugation for amphiphilic PVDF/F127-g-(HFBM)₈~DMAC membrane (Figure 1 (1)) increased obviously. The results may further demonstrate the more pronounced surface enrichment of low surface energy fluorine-containing blocks on amphiphilic PVDF/F127-g-(HFBM)₈~DMAC membrane surface compared with that on the hydrophilic PVDF/F127-g-(DFHM)₈~DMAC membrane surface.

From this perspective, the ternary amphiphilic copolymer conformation rendered an elegant surface architecture control and accomplished the switcheroe of membrane surfaces between amphiphilic and hydrophilic surfaces without any changes of the constituents in the membrane formation recipe.

Regulation via Solvent Volatility. The selectivity of solvent in the casting solution was another crucial parameter for manipulating

the microphase separation of the amphiphilic copolymers and subsequent surface segregation during the wet phase inversion process.^{22,23} Here, THF and DMAC mixed solvent with a weight ratio of 1:4 were introduced in the hope of enhancing the surface enrichment of PDFHM blocks. THF was a highly volatile solvent with a boiling point of 65.4 °C under ambient pressure and δ value of about 9.2 (cal/cm²)⁻³. According to the solubility parameter theory, the mixed solvent may not change the structures of the F127-g-(DFHM)_n cluster greatly. However, before immersion into the nonsolvent bath, THF was allowed to evaporate for a certain period, which would definitely affect the surface segregation behavior of the copolymers: owing to the high evaporation rate of THF, the freezing of polymer solution was accelerated and surface enrichment of flexible short-chain PDFHM blocks was reinforced.¹⁹

Figure 1 (c) displayed the XPS C1s core level spectra resolving results of PVDF/F127-g-(DFHM)₈~DMAC and THF membranes, and the corresponding surface coverage ratios were listed in Table 1, entries 10–13. The surface coverage of low surface energy PDFHM blocks were obviously increased compared with that of PVDF/F127-g-(DFHM)_n~DMAC membranes; moreover surface coverage of hydrophilic PEO blocks was retained at a relative high level. The maximal Φ_{DFHM} and Φ_{PEO} values were 33.5% and 30.2%, respectively. The AFM phase image of PVDF/F127-g-(DFHM)₈~DMAC and THF membrane surface was presented in Figure 1(3). As predicted, the surface corrugation increased compared with that of the hydrophilic PVDF/F127-g-(DFHM)₈~DMAC membrane surface. All the above phenomena validated the construction of amphiphilic surfaces for PVDF/F127-g-(DFHM)_n~DMAC and THF membranes.

3.3. Versatile Antifouling Properties. Generally, higher surface hydrophilicity or oleophobicity signified more robust fouling resistant or fouling release (for oily foulants especially) attributes. In our study, the surface hydrophilicity/oleophobicity was evaluated by water (CA_w) and oil (CA_o) contact angle measurement (see Figure S4 (a-c), Supporting Information). For the amphiphilic PVDF/F127-g-(HFBM)_n~DMAC and PVDF/F127-g-(DFHM)_n~DMAC and THF membrane, the simultaneous surface enrichment of hydrophilic and low surface energy blocks did not largely influence the membrane surface hydrophilicity. Meanwhile, CA_o was increased obviously compared with that of the control PVDF membrane, indicating an improved fouling release potential. For hydrophilic PVDF/F127-g-(DFHM)_n~DMAC membrane surfaces, both the CA_w and CA_o values changed slightly. The CA_w of the hydrophilic PVDF/F127-g-(DFHM)_n~DMAC membrane was around 90°, which may be explained by the intrinsic high water contact angle of the PVDF matrix material and the influence of surface roughness as well.

The membrane surface free energy (γ), as well as dispersive (γ_s^{LW}) and polar (γ_s^{AB}) components, was analyzed using the three-liquid Lifshitz-van der Waals acid–base model. Compared with control PVDF membrane, γ , along with γ_s^{LW} and γ_s^{AB} , of amphiphilic PVDF/F127-g-(HFBM)_n~DMAC and PVDF/F127-g-(DFHM)_n~DMAC and THF membrane surfaces exhibited dramatically decreasing trends (see Figure S4 (1–3), Supporting Information), with the lowest value of about 25 mN/m, hinting a desirable fouling release potential.²⁴ Furthermore, the lower surface free energy or the higher CA_o value reflected a preferable oil-repellent ability. However, γ of hydrophilic PVDF/F127-g-(DFHM)_n~DMAC membrane surfaces still retained at the similar high level compared with that of the control PVDF

membrane surfaces. All the above phenomena were in a pretty good agreement with the contact angle, XPS and AFM measurement results.

The filtration performance including the permeation, retention, and antifouling properties of the as-prepared membranes was investigated in a dead-end filtration module employing oil/water emulsion and BSA aqueous solution as model systems, two kinds of the representative foulants in the water treatment and reclamation industries. The operation process mainly included three steps: first-round pure water filtration, feed solution filtration, and the second-round pure water filtration after simple hydraulic washing for the membranes, the membrane fluxes, including J_{w1} , J_p , and J_{w2} , were measured, respectively. The whole filtration process was carried out under the same near-surface agitating speed of 200 rpm.

Analysis of the time-dependent flux variations during the filtration process allowed for determination of several evaluating parameters, which were defined as total flux decline ratio (DR_t), reversible flux decline ratio (DR_r), irreversible flux decline ratio (DR_{ir}), and flux recovery ratio (FRR) calculated by the following equations

$$DR_t = 1 - J_p/J_{w1}$$

$$DR_r = (J_{w2} - J_p)/J_{w1}$$

$$DR_{ir} = 1 - J_{w2}/J_{w1}$$

$$FRR = J_{w2}/J_{w1}$$

During the pressure-driven dynamic membrane filtration process, the irreversible flux decline was mainly caused by the direct attachment and subsequent intractable adsorption of foulants on membrane surface or foulants blockage inside the membrane pores, which were extremely difficult or impossible to recover. The reversible flux decline was dominantly attributed to the reversible foulant deposition, which could be simply recovered by hydraulic washing and probably released from membrane surface with the assistance of near-surface agitation. Obviously, DR_t was the sum of DR_{ir} and DR_r . FRR was the difference between 1 and DR_{ir} ; therefore, lower DR_{ir} meant higher FRR .

Figure 2 (a-c) presents the time-dependent permeation flux variations of the membranes with oil/water emulsion as model foulant, and the corresponding DR_t , DR_{ir} , DR_r , and FRR values were plotted as functions of the Φ_{HFBM}/Φ_{DFHM} and Φ_{PEO} values (Figure 2 (d)). Obviously, the water permeation flux of control PVDF membrane was dramatically decreased and water flux of the refreshed membrane was slightly recovered, the corresponding DR_t was as high as about 75.0% (DR_r about 30.5%, DR_{ir} about 44.5%), and the FRR value was as low as 55.5%. It was demonstrated that the irreversible flux decline and flux recovery property were predominantly dependent on the surface coverage of hydrophilic blocks. In detail, the DR_{ir} values were remarkably decreased with the increase of Φ_{PEO} and kept lower than 5.0% (corresponding FRR values higher than 95.0%) when Φ_{PEO} was ascended above 20.0%. However, the remarkable alleviation of reversible flux decline required the simultaneous enhancement of surface coverage of hydrophilic and low surface energy blocks. The DR_r value was finally reached at a minimum level of about 5.3% with sufficiently high Φ_{PEO} and $\Phi_{HFBM}(\Phi_{DFHM})$ values, e.g., 39.4% and 30.6% on amphiphilic PVDF/F127-g-(HFBM)₈~DMAC or 33.5% and 30.2% on

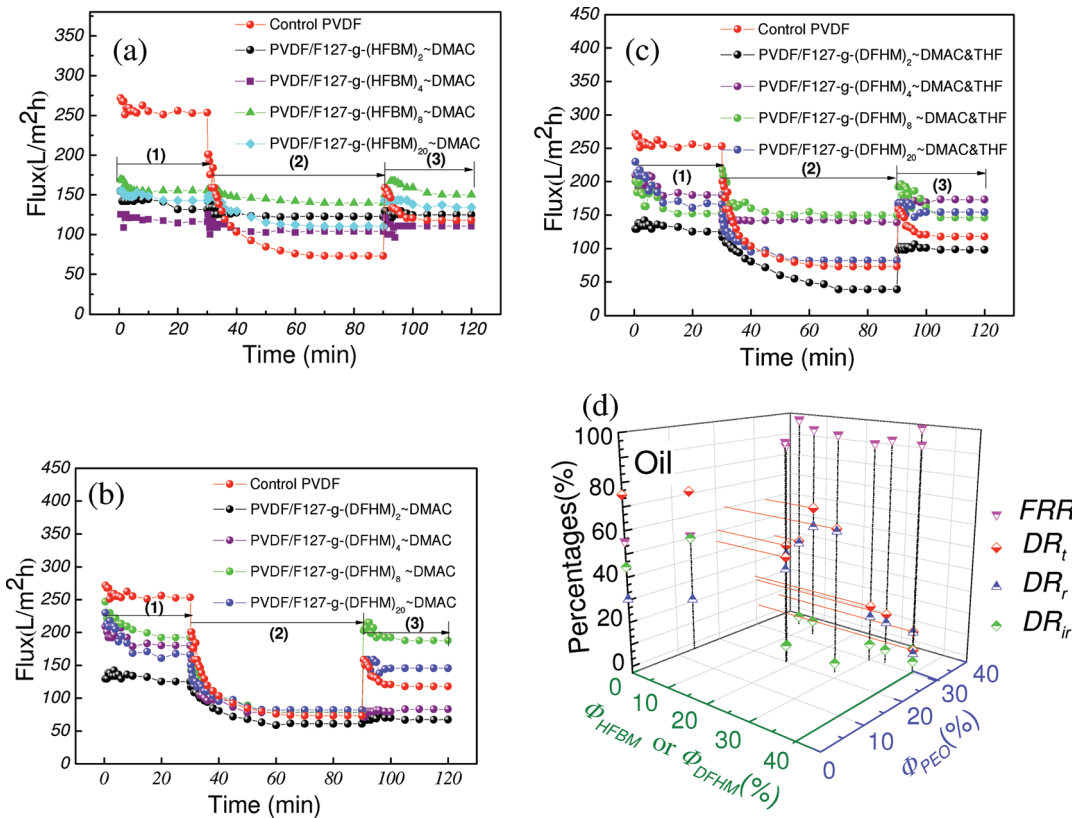


Figure 2. Time-dependent water permeation flux during oil/water emulsion filtration of (a) PVDF/F127-g-(HFBM)_n~DMAC, (b) PVDF/F127-g-(DFHM)_n~DMAC, and (c) PVDF/F127-g-(DFHM)_n~DMAC and THF membranes and (d) a summary of the corresponding DR_t , DR_r , DR_{ir} , and FRR values as functions of Φ_{HFBM} (Φ_{DFHM}) and Φ_{PEO} values. The operation process included three steps: pure water filtration (1), oil/water emulsion filtration (2), 20 min of water washing (not shown) and the second-round pure water filtration (3).

amphiphilic PVDF/F127-g-(DFHM)₈~DMAC and THF membrane surfaces. Finally, these amphiphilic membrane surfaces exhibited only 6.8% total flux decline and more than 99.0% permeation flux recovery. It should be mentioned that the oil retention ratio determined by UV-visible spectrometry was all higher than 99.0%. The turbidity was decreased from 190.7 NTU of feed solution to only 11.4 NTU of the permeate. All the amphiphilic membranes exhibited preferential COD retention ratio of higher than 99.5%, and the COD value of the permeate was about 10 ppm, meeting the O&G standards for direct discharge.

The time-dependent permeation flux variations of the membranes with BSA aqueous solution as model foulant system were presented in Figure 3 (a-c). The control PVDF membrane underwent serious permeation flux decline and poor flux recovery: DR_t as high as about 76.1% (DR_r about 48.8%, DR_{ir} about 27.3%) and FRR values as low as 55.5%. As shown in Figure 3 (d), both the irreversible flux decline (or flux recovery property) and reversible flux decline were mainly dependent on the surface coverage of hydrophilic blocks but less influenced by the surface coverage of the low surface energy blocks: as long as Φ_{PEO} were above 20.0% and 32.0%, both DR_{ir} and DR_r would remain less than 5.0% and 20.0%, respectively, regardless of the Φ_{HFBM} (Φ_{DFHM}). Finally, the hydrophilic PVDF/F127-g-(DFHM)₂₀~DMAC membrane surfaces exhibited only 17.0% total flux decline and more than 99.0% permeation flux recovery. The BSA retention ratio of all the modified membranes determined by UV-visible spectrometry was about $50.5 \pm 3.5\%$, which may be attributed to the

slightly varied skin pore size (see Figure S2 (1–3), Supporting Information). The COD value was decreased from 1487 ppm of feed solution to about 705 ppm of the permeate, while turbidity was decreased from about 3.7 to 1.7 NTU. The retention for the proteins-containing wastewater was not sufficient for reuse or discharge; however, such hydrophilic membrane may be applicable for pretreatment of reverse osmosis process. It should be mentioned that the separation performance of the modified PVDF membranes was competitive compared with commercially available PVDF membranes.

Moreover, after three times membrane filtration, the antifouling properties of the hydrophilic or amphiphilic membrane surfaces still maintained at a high level (see Figure S5, Supporting Information). It may be explained by one of the inherent self-healing capability of surface segregation methods: the fouling-resistant layer lost from the surface during operation or cleaning can be substantially replenished by the spontaneous segregation of the additives underneath.

A tentative antifouling mechanism has been proposed in our previous study.⁹ Herein, a complementary mechanism was tentatively put forward. The hydrophilic antifouling surfaces can bind amounts of water molecules and generate steric hydration defense layers for suppressing the nonspecific interaction between foulants and surfaces through the “hydration pressure” or “hydrophilic repulsion”, thus endowing the surfaces with outstanding fouling resistant potential. During the dynamic filtration process, the synergy of hydration layer on membrane surface and “water corona”²⁵ around protein molecules deter the conformational

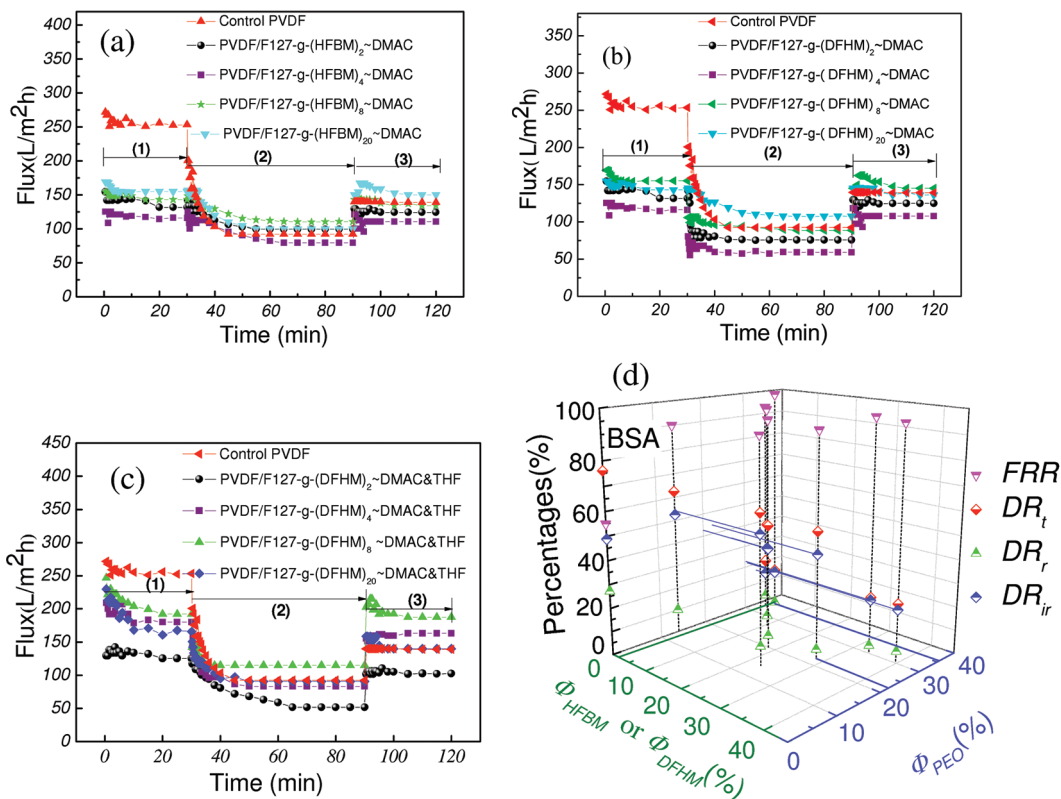


Figure 3. Time-dependent water permeation flux during BSA aqueous solution filtration of (a) PVDF/F127-g-(HFBM)_n~DMAC, (b) PVDF/F127-g-(DFHM)_n~DMAC, and (c) PVDF/F127-g-(DFHM)_n~DMAC and THF membranes and (d) a summary of the corresponding DR_t , DR_r , DR_{ir} , and FRR values as functions of $\Phi_{HFBM}(\Phi_{DFHM})$ and Φ_{PEO} values. The operation process included three steps: pure water filtration (1), BSA aqueous solution filtration (2), 20 min of water washing (not shown) and the second-round pure water filtration (3).

transformations of proteins, dramatically reducing or even eliminating the irreversible flux decline. The amphiphilic antifouling surfaces bearing mixed brush architecture comprised both hydrophilic blocks and low surface energy blocks. Hydrophilic blocks generated fouling resistant hydration layers; whereas low surface energy blocks formed amounts of nonadhesive microdomains randomly distributing on membrane surfaces, which played major role in evicting foulants away from the surfaces, thus endowing the surfaces with outstanding fouling release potential. During the dynamic filtration process, the fouling resistant ability impeded the irreversible flux decline; the fouling release ability prevented coalescence, migration, and spreading of the holistic hydrophobic oil droplets, remarkably reducing or even eliminating the reversible flux decline.

In summary, a facile approach for constructing tunable hydrophilic or amphiphilic antifouling membrane surfaces was developed for combating different surface foulants during the water treatment. Ternary amphiphilic copolymers bearing strong solvophilicity, low surface energy block, or casting solvent with high volatility favored the construction of amphiphilic antifouling surfaces, which exhibited superior antifouling performance for oily foulants. In sharp contrast, ternary amphiphilic copolymers bearing weak solvophilicity, low surface energy block, or casting solvent with low volatility favored the construction of hydrophilic antifouling surfaces, which exhibited superior antifouling performance for biofoulants.

ASSOCIATED CONTENT

Supporting Information. Detailed experimental methods, FTIR and ¹H NMR spectra for amphiphilic copolymers,

SEM morphologies of membranes, schematic illustrations of the microphase separation and surface segregation behavior of the amphiphilic copolymers, water/oil contact angles and surface free energy parameters of membrane surfaces are provided. This material is available free of charge via the Internet at <http://pubs.acs.org>.

AUTHOR INFORMATION

Corresponding Author

*E-mail: zhyjiang@tju.edu.cn.

ACKNOWLEDGMENT

The authors thank financial support from the Drug Separation and Purification Project in Programme for Development of Novel Drug and the Program of Introducing Talents of Discipline to Universities (No. B06006).

REFERENCES

- Shannon, M. A.; Bohn, P. W.; Elimelech, M.; Georgiadis, J. G.; Marinas, B. J.; Mayes, A. M. Science and technology for water purification in the coming decades. *Nature* **2008**, *452* (7185), 301–310.
- Zhao, D. Y.; Jaroniec, M.; Hsiao, B. S. Editorial for themed issue on “Advanced Materials in Water Treatments”. *J. Mater. Chem.* **2010**, *20* (22), 4476–4477.
- Mayes, A. M.; A., A. Oil industry wastewater treatment with fouling resistant membranes containing amphiphilic comb copolymers. *Environ. Sci. Technol.* **2009**, *43* (12), 4487–4492.

- (4) Zhou, M.; Liu, H.; Kilduff, J. E.; Langer, R.; Anderson, D. G.; Belfort, G. High-throughput membrane surface modification to control NOM fouling. *Environ. Sci. Technol.* **2009**, *43* (10), 3865–3871.
- (5) Freeman, B. D.; Ju, H.; McCloskey, B. D.; Sagle, A. C.; Wu, Y. H.; Kusuma, V. A. Crosslinked poly(ethylene oxide) fouling resistant coating materials for oil/water separation. *J. Membr. Sci.* **2008**, *307* (2), 260–267.
- (6) Wang, X. F.; Chen, X. M.; Yoon, K.; Fang, D. F.; Hsiao, B. S.; Chu, B. High flux filtration medium based on nanofibrous substrate with hydrophilic nanocomposite coating. *Environ. Sci. Technol.* **2005**, *39* (19), 7684–7691.
- (7) Huang, H.; Young, T. A.; Jacangelo, J. G. Unified membrane fouling index for low pressure membrane filtration of natural waters: principles and methodology. *Environ. Sci. Technol.* **2007**, *42* (3), 714–720.
- (8) Yamamura, H.; Kimura, K.; Okajima, T.; Tokumoto, H.; Watanabe, Y. Affinity of functional groups for membrane surfaces: implications for physically irreversible fouling. *Environ. Sci. Technol.* **2008**, *42* (14), 5310–5315.
- (9) Chen, W.; Su, Y.; Peng, J.; Dong, Y.; Zhao, X.; Jiang, Z. Engineering a robust, versatile amphiphilic membrane surface through forced surface segregation for ultralow flux-decline. *Adv. Funct. Mater.* **2011**, *21* (1), 191–198.
- (10) Wang, Y. Q.; Wang, T.; Su, Y. L.; Peng, F. B.; Wu, H.; Jiang, Z. Y. Remarkable reduction of irreversible fouling and improvement of the permeation properties of poly(ether sulfone) ultrafiltration membranes by blending with pluronic F127. *Langmuir* **2005**, *21* (25), 11856–11862.
- (11) Hester, J. F.; Mayes, A. M. Design and performance of foul-resistant poly(vinylidene fluoride) membranes prepared in a single-step by surface segregation. *J. Membr. Sci.* **2002**, *202* (1–2), 119–135.
- (12) Banerjee, I.; Pangule, R. C.; Kane, R. S. Antifouling coatings: recent developments in the design of surfaces that prevent fouling by proteins, bacteria, and marine organisms. *Adv. Mater.* **2011**, *23* (6), 690–718.
- (13) Chelmowski, R.; Koster, S. D.; Kerstan, A.; Prekelt, A.; Grunwald, C.; Winkler, T.; Metzler-Nolte, N.; Terfort, A.; Woll, C. Peptide-based SAMs that resist the adsorption of proteins. *J. Am. Chem. Soc.* **2008**, *130* (45), 14952–14953.
- (14) Statz, A. R.; Meagher, R. J.; Barron, A. E.; Messersmith, P. B. New peptidomimetic polymers for antifouling surfaces. *J. Am. Chem. Soc.* **2005**, *127* (22), 7972–7973.
- (15) Holmlin, R.; Chen, X.; Chapman, R.; Takayama, S.; Whitesides, G. Zwitterionic SAMs that resist nonspecific adsorption of protein from aqueous buffer. *Langmuir* **2001**, *17* (9), 2841–2850.
- (16) Dalsin, J. L.; Messersmith, P. B. Bioinspired antifouling polymers. *Mater. Today* **2005**, *8* (9), 38–46.
- (17) Jiang, S.; Cao, Z. Ultralow-fouling, functionalizable, and hydrolyzable zwitterionic materials and their derivatives for biological applications. *Adv. Mater.* **2009**, *21*, 1–13.
- (18) Adout, A.; Kang, S.; Asatekin, A.; Mayes, A. M.; Elimelech, M. Ultrafiltration membranes incorporating amphiphilic comb copolymer additives prevent irreversible adhesion of bacteria. *Environ. Sci. Technol.* **2010**, *44* (7), 2406–2411.
- (19) Peinemann, K. V.; Abetz, V.; Simon, P. F. W. Asymmetric superstructure formed in a block copolymer via phase separation. *Nat. Mater.* **2007**, *6* (12), 992–996.
- (20) Schacher, F.; Ulbricht, M.; Müller, A. Self-Supporting, double stimuli-responsive porous membranes from polystyrene-block-poly(*N*, *N*-dimethylaminoethyl methacrylate) diblock copolymers. *Adv. Funct. Mater.* **2009**, *19* (7), 1–6.
- (21) Grubbs, R. B. Nanoparticle assembly -Solvent-tuned structures. *Nat. Mater.* **2007**, *6* (8), 553–555.
- (22) Nie, Z. H.; Fava, D.; Kumacheva, E.; Zou, S.; Walker, G. C.; Rubinstein, M. Self-assembly of metal-polymer analogues of amphiphilic triblock copolymers. *Nat. Mater.* **2007**, *6* (8), 609–614.
- (23) Kriksin, Y. A.; Khalatur, P. G.; Erukhimovich, I. Y.; ten Brinke, G.; Khokhlov, A. R. Microphase separation of diblock copolymers with amphiphilic segment. *Soft Matter* **2009**, *5* (15), 2896–2904.
- (24) Krishnan, S.; Weinman, C. J.; Ober, C. K. Advances in polymers for anti-biofouling surfaces. *J. Mater. Chem.* **2008**, *18* (29), 3405–3413.
- (25) Nel, A. E.; Madler, L.; Velegol, D.; Xia, T.; Hoek, E. M. V.; Somasundaran, P.; Klaessig, F.; Castranova, V.; Thompson, M. Understanding biophysicochemical interactions at the nano-bio interface. *Nat. Mater.* **2009**, *8* (7), 543–557.